Sequential Stochastic Response Surface Method Using Moving Least Squares Based Sparse Grid Scheme for Efficient Reliability Analysis

Amit Kumar Rathi[1], Sudhi Sharma P V[2] and Arunasis Chakraborty[1,a)]

[1]Department of Civil Engineering, Indian Institute of Technology Guwahati, Assam 781039, India

[2]Bentley Systems India Pvt. Ltd., Kolkata, WB 700156, India

[a)]Presenting & corresponding author: arunasis@iitg.ernet.in

ABSTRACT

Present work demonstrates an efficient method for reliability analysis using sequential development of the stochastic response surface in sparse grid framework. Here, stochastic response surface is formed by orthogonal Hermite polynomial basis, whose unknown coefficients are evaluated using moving least squares technique. To construct the response surface, collocation points (as in the conventional stochastic response surface method (SRSM)) are replaced by the sparse grid scheme that reduces the number of function evaluations. Additionally, the sparse grid is populated sequentially based on the optimization process for finding the most probable failure point. After constructing the sequential SRSM, reliability analysis is conducted using importance sampling. Numerical study shows the efficiencies of the proposed sequential SRSM in terms of accuracy and number of time-exhaustive evaluation of the original performance function.

Keywords: Reliability Analysis, Polynomial Chaos Expansion, Moving Least Squares, Hermite Polynomial, Sparse Grid.

Introduction

Surrogate modelling has become an important numerical tool in the recent past for various engineering applications like optimization [1], reliability analysis [2] [3], uncertainty quantification [4]. However, this approximate modelling is not always convergent and may yield significant modelling error [3][5]. One of the method is polynomial chaos expansion (PCE) [2] which can be used for complex scientific and engineering problems. Using PCE, Isukapalli [6] proposed stochastic response surface method (SRSM) to approximate the performance function. Formation of the SRSM is done using the actual function evaluations at Gauss quadrature points (a.k.a. collocation points) to determine the unknown coefficients by regression. The method proves to be robust and stable as it uses regression and orthogonal polynomials (i.e. Hermite polynomial) making it convergent in L^2 sense [2]. Later, Xiu and Karniadakis [4] proposed generalized PCE formulation for solving stochastic differential equations using the Askey polynomial scheme. Application of this method have been studied for various engineering problems like foundation on heterogeneous soil, aircraft joined-wing structure and so on [7][8]. Sudret and Der Kiureghian [7] proposed an application of PCE along with first order reliability method (FORM) and importance sampling technique for solving random field problems. Similar effort has been made by Kameshwar *et al.* [5] to combine PCE with FORM for reliability analysis. They substituted the individual contribution of the random variables in limit state by unidimensional Hermite polynomials which is later solved for reliability index. Gavin and Yau [9] proposed a higher order SRSM (HO-SRSM) using Chebyshev polynomials in which the polynomial order with respect to individual random variable is determined based on the significance of the respective polynomial coefficients.

Apart from using regression analysis which is a widely accepted tool for determining the unknown coefficients in SRSM, advanced techniques like least angle regression (LARS) [10], moving least squares (MLS) [11] and so on, have been adopted for improving the accuracy of the stochastic response surface approximation. However, MLS based SRSM can give inaccurate estimation of failure probability in some cases as shown by Xiong *et al.* [12]. They suggested a double weighted strategy where extra weightage is imposed on the support points near the limit state for better local approximation of SRSM.

Although SRSM is considered to be accurate but it suffers from substantial increase in the number of actual function calls with the increase of number of random variables (i.e. *curse of dimensionality*). This, in turn, makes the process computationally exhaustive and inefficient. To counter this issue, Blatman and Sudret [10] proposed hyperbolic PCE with LARS. Another technique is adaptive-sparse PCE method [13] where the insignificant terms in the bivariate polynomial expansion are dropped. However, the literatures still lack in limiting the number and the location of support points which affects the overall performance to replicate the original surface.

With this in view, present work suggests an efficient method for reliability assessment for large field problem. A sequential algorithm for SRSM is presented to address the curse of dimensionality. The stochastic response surface is formed using the Hermite polynomial basis function. The unknown coefficients of the response surface are evaluated by MLS technique. For constructing the response surface, collocation points (as in the conventional SRSM) are replaced by the sparse grid scheme which reduces the function evaluations. Additionally, the sparse grid is populated sequentially based on the optimization process for finding the most probable failure point. Once the sequential SRSM is formed, importance sampling is adopted for reliability evaluation.

MLS based SRSM

In stochastic response surface method, the original performance function is replaced by a summation of orthogonal polynomial described in terms of the random variables. Different orthogonal polynomials are described in the literature (e.g. Legendre, Laguerre, Hermite, Chebyshev) for different applications. Off all these polynomials, Hermite polynomial is popular in reliability analysis and stochastic finite element modelling. Mathematically, Hermite polynomial of order o can be expressed as [6]

$$\Gamma_o(\xi_{i_1}, \xi_{i_2}, \ldots, \xi_{i_o}) = e^{\frac{1}{2}\xi^T\xi}(-1)^o \frac{\partial^o e^{-\frac{1}{2}\xi^T\xi}}{\partial\xi_{i_1}\partial\xi_{i_2}\ldots\partial\xi_{i_o}}. \tag{1}$$

where, $\xi = \{\xi_1\ \xi_2\ \ldots\ \xi_n\}^T$ denotes the vector of standard normal random variables. Thus, using polynomial of a predefined order o, the original performance function can be expressed as

$$y(\xi) = \alpha_0 + \sum_{i_1=1}^{n} \alpha_{i_1}\Gamma_1(\xi_{i_1}) + \sum_{i_1=1}^{n}\sum_{i_2=1}^{i_1} \alpha_{i_1 i_2}\Gamma_2(\xi_{i_1}, \xi_{i_2}) + \ldots + \sum_{i_1=1}^{n}\sum_{i_2=1}^{i_1}\cdots\sum_{i_o=1}^{i_{o-1}} \alpha_{i_1 i_2 \ldots i_o}\Gamma_o(\xi_{i_1}, \xi_{i_2}, \ldots, \xi_{i_o}). \tag{2}$$

The unknown coefficients of the aforementioned equation can be denoted by $\mathbf{b} = \{\alpha_0\ \alpha_1\ \ldots\ \alpha_n\ \alpha_{11}\ \alpha_{21}\ \ldots\ \alpha_{nn\ldots n}\}^T$. Thus, rewriting the Eq. 2 in simplified matrix form, one gets

$$y(\xi) = \Xi(\xi)\mathbf{b} \tag{3}$$

where, $\Xi(\xi)$ consists of the Hermite polynomial basis of order $\leq o$. A total of $n_b = \frac{(n+o)!}{n!\,o!}$ coefficients need to be determined in the representation of SRSM. Usually, these unknown coefficients $\mathbf{b}$ are evaluated using regression analysis [6]. However, a global approximation of the original performance function often lead to large error as it fails to capture local variations, if any [14]. To address this problem, moving least square (MLS) based regression is often prescribed in the literature where the unknown coefficients change with locations (i.e. support points). Using this modified regression technique, the unknown coefficients $\mathbf{b}$ can be expressed as follows [15]

$$\mathbf{b} = [\mathbf{\Xi}^{\mathrm{T}}\,\mathbf{W}\,\mathbf{\Xi}]^{-1}\,[\mathbf{\Xi}^{\mathrm{T}}\,\mathbf{W}]\,\mathbf{y} \tag{4}$$

where, the actual values of the performance function evaluated at the support points are expressed by the vector $\mathbf{y}$. Also, each row of the matrix $\mathbf{\Xi}$ represents the polynomial basis corresponding to the location. The weight matrix $\mathbf{W}$ in the above equation consists of weight function w which is given by [15]

$$w(\delta) = \begin{cases} \frac{\bar{w}(\delta)}{\sum_{i=1}^{k}\bar{w}(\delta_i)} & \text{if } \delta \leq r \\ 0 & \text{elsewhere} \end{cases} \tag{5}$$

where,

$$\bar{w}_i(\delta) = \frac{\{(\frac{\delta}{r})^2 + \epsilon\}^{-2} - (1+\epsilon)^{-2}}{\epsilon^{-2} - (1+\epsilon)^{-2}} \tag{6}$$

In the above equation, δ represents the Euclidian distance between the respective support point, r is the influence radius of the weight function and ϵ is adopted as 10^{-5} [15] [14]. Although, this evolving regression technique improves the performance of the meta model significantly, it still suffers computational challenges in problems with large dimensions and multiple optima. Besides this, computational cost for problem with large dimension has remained a major challenge to the designers. Thus, there is a constant demand for a more efficient technique for reliability estimation that involves less functional evaluations and subsequent computational cost without compromising with the quality of the end results. With this in view, present study aims to demonstrate sequential development of stochastic response method where the support points are generated using sparse grid technique.

Proposed Sequential SRSM with Sparse Grid Scheme

In this section, the details of the proposed sequential stochastic response surface using MLS based PCE in sparse grid scheme is presented.

Sequential SRSM

As in the Eq. 2, stochastic response surface is constructed by Hermite polynomial basis with unknown coefficients. To evaluate these coefficients, support points are generated using different techniques namely collocation method, Latin hypercube design, monomial cubature rule among many others [11]. The location of these points are known prior to the determination of the coefficients for constructing the polynomial basis matrix $\boldsymbol{\Xi}$. Hence, the number of support points n_e should be at least equal to the number of unknown coefficient (i.e. n_b). Thus, the support points generation scheme can be dense or sparse depending on various issues like number of random variables n and order of the polynomial o. In case of dense generation, computation cost rises making SRSM less effective whereas the sparse population of support points might lead to inaccurate approximation. Additionally, for an ideal situation in reliability analysis, more support points are required in the vicinity of the limit state (i.e. $y(\mathbf{x}) = 0$). As these points account for better approximation and accuracy in estimation of probability of failure [12]. Therefore, customizing the number of support points n_e in a single go based on o, n etc. becomes a difficult task. To overcome this problem, the present study uses an iterative scheme where the support points are generated only in the vicinity where it is required. This is done by optimizing the Gaussian space of the approximated surface to find the most probable failure point (or design point) as

$$\begin{array}{ll} \text{Find :} & \xi \\ \text{Minimize :} & |\xi|_2 \\ \text{Subjected to :} & \tilde{y}(\mathbf{x}) = 0. \end{array} \tag{7}$$

Above optimization is executed over the approximated surface [i.e. $\tilde{y}(\,.\,)$] which imposes no restriction on the choice of the optimization tool. Hence, different searching tools like gradient based methods, genetic algorithm can be adopted to perform the constrained optimization. Thus, the accuracy of the optimization largely depends on the accuracy of the meta modelling. Although, the accuracy of the meta model increases with number of support points, a tradeoff between the number of points and modelling error is adopted to optimize computational cost. In this study, sequential quadratic programming (SQP) inbuilt in MATLAB® [16] is adopted for solving the Eq. 7 to evaluate the design point ξ^* in the Gaussian space.

From the above discussion, it is evident that the ideal condition requires more points in the failure region and less points elsewhere. This, in turn, improves the efficiency of the reliability method by limiting the number of function calls in order to reduce cost of computation. To explain this phenomenon, Fig. 1 demonstrates the points generated by the full grid formation using the collocation method. These points almost uniformly cover the domain with increase in the order o of PCE, especially the domain with high probability [11]. This might lead to inclusion of points that are insignificant for estimation of probability of failure and lead to excessive computational burden. Whereas the points generated by the sparse grid scheme are selective which is explained later.

Thus, to minimize the function calls (in other words, the number of support points), the proposed method initiates at a predefined point. Without loss of generality, this initial design point is considered as the mean values of the random variables (i.e. $\mu_{\mathbf{X}}$). The support points are allocated around this design point, preferably with the extent to incorporate the failure region (i.e. $y(\mathbf{x}) \leq 0$). PCE is constructed using Eq. 2 of order o for n random variables. In this context, the number of support points must be $\geq n_b$ for solving the PCE based approximation by MLS technique as explained in the Eq. 4. After constructing the approximated surface $\tilde{y}(\mathbf{x})$, constrained optimization problem as explained in Eq. 7 is solved to identify the failure region and the corresponding new optima. This new deign point is further used for generating more support points as explained earlier for the following iteration. In order to generate more support points in the area near the limit state, the spatial extent of the generated support

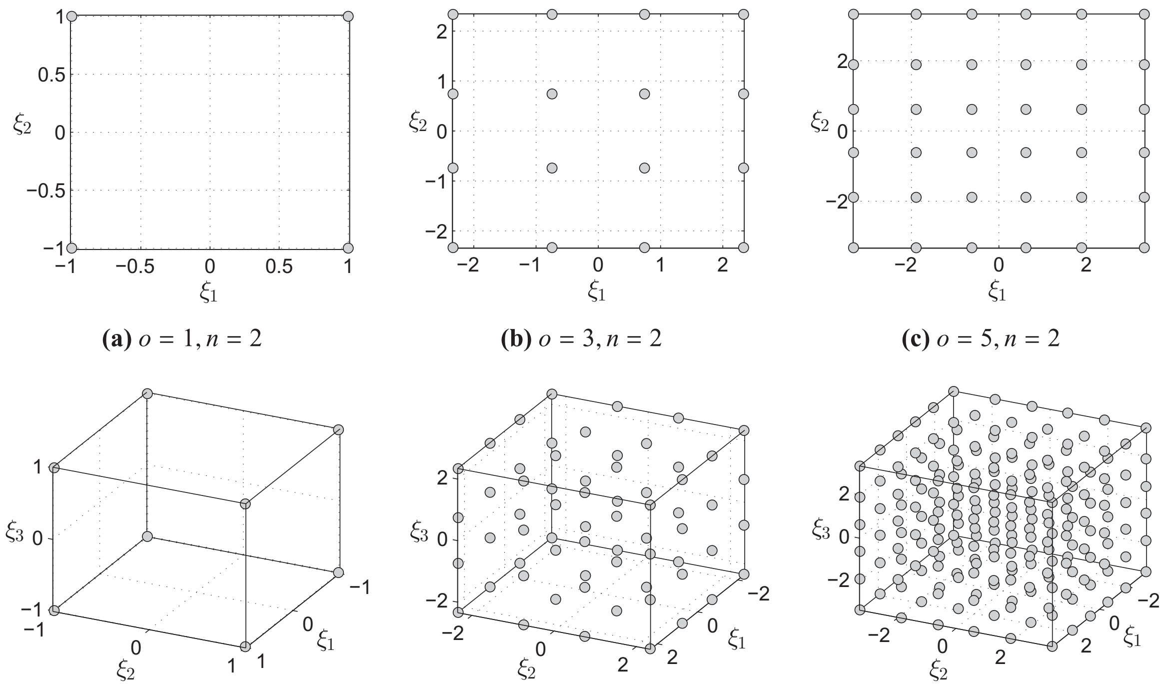

(a) $o = 1, n = 2$ **(b)** $o = 3, n = 2$ **(c)** $o = 5, n = 2$

(d) $o = 1, n = 3$ **(e)** $o = 3, n = 3$ **(f)** $o = 5, n = 3$

Figure 1: Collocation points with different order and dimension

points in every iteration *it* is reduced by factor λ ($\lambda < 1.0$). The value of this reduction factor depends on the required convergence speed and the accuracy to be attained. After every iteration, convergence of the solution is checked by $|\tilde{y}(\mathbf{x}^*)_{it-1} - \tilde{y}(\mathbf{x}^*)_{it}| \leq \breve{e}_1$ and $|\mathbf{x}^*_{it-1} - \mathbf{x}^*_{it}| \leq \breve{e}_2$, where $\breve{e}_1$ and $\breve{e}_2$ are the permissible errors of order, typically in the range of $10^{-2} - 10^{-3}$. Once the convergence is achieved, reliability analysis is conducted using importance sampling method as explained later in this section. The proposed sequential SRSM provides the information of the most probable failure point $\mathbf{x}^*$ and the probability of failure p_f associated with it.

Sparse Grid Scheme

The proposed method employs sparse grid scheme where support points are judiciously selected from the full grid. The sparse grid formation follows Smolyak's algorithm which includes the points from the lower product grids [17] and is controlled by a factor l such that

$$SG_l = \sum_{\sum_{i=1}^{m} i_j \leq l+m-1} (\Delta^{i_1} \otimes \Delta^{i_2} \otimes \cdots \otimes \Delta^{i_m})(y) \tag{8}$$

where, this factor l is the level of the sparse grid scheme. In Eq. 8, Δ represents the unidimensional difference quadrature term defined in the unit space i.e. [0, 1]. Present study uses an equidistant sparse grid scheme as proposed by Clenshaw and Curtis [18]. The number of points generated by this scheme in unidimensional direction is given by [19]

$$n_{c,i} = \begin{cases} 1 & \text{if } i = 1 \\ 2^{i-1} + 1 & \text{if } i > 1 \end{cases} \tag{9}$$

where, i denotes a positive integer like 1, 2, 3, ... The coordinates of these points in the unit space is obtained from [19]

$$x_k^{i,j} = \begin{cases} 0.5 & \text{for } j = 1 \text{ if } n_{c,i} = 1 \\ \frac{j-1}{n_{c,i}-1} & \text{for } j = 1, 2, \ldots, n_{c,i} \text{ if } n_{c,i} > 1 \end{cases} \tag{10}$$

where, $x_k^{i,j}$ represents the set of coordinates for the k^{th} random variable. Fig. 2 shows the Clenshaw-Curtis sparse grid generated for various l values. In contrary to the collocation points which is a full grid scheme as shown in

Fig. 1, sparse grid scheme fills the domain (in this case it is a unit space) non-uniformly. Thus, creating large voids between adjacent points. The proposed sequential method in this study attempts to fill such voids in the vicinity of critical regions of the limit state only.

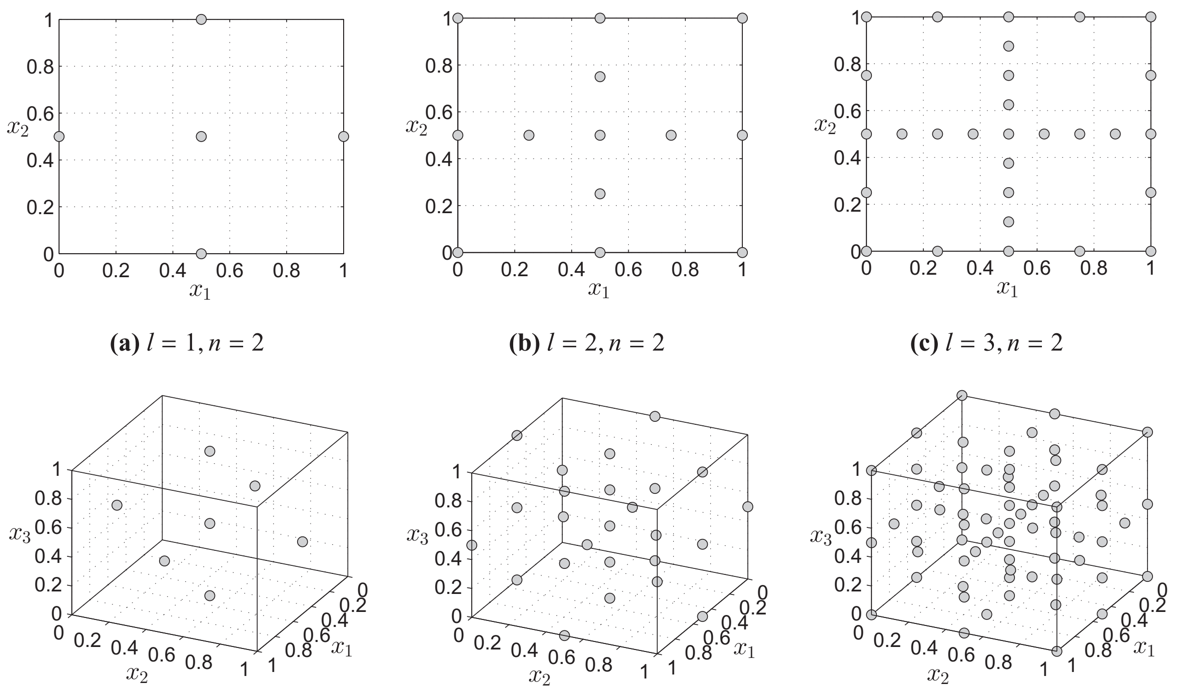

(a) $l = 1, n = 2$ **(b)** $l = 2, n = 2$ **(c)** $l = 3, n = 2$

(d) $l = 1, n = 3$ **(e)** $l = 2, n = 3$ **(f)** $l = 3, n = 3$

Figure 2: Support points generated by Clenshaw-Curtis sparse grid scheme

Reliability Assessment

After satisfying convergence criteria, reliability analysis is conducted for estimating the probability of failure p_f. Based on the support points generated sequentially in the iterative manner, approximate surface $\tilde{y}(\mathbf{x})$ is constructed. In this context, it may be noted that support points generated in every iteration along with the corresponding values of the original function are saved to construct the global response surface. Using this global response surface, proposed method estimates the most probable failure point $\mathbf{x}^*$. Here, importance sampling is chosen with sample size (say 10^3 or 10^4) for conducting the reliability assessment in this study. The probability of failure p_f is calculated as [20]

$$p_f \approx \frac{1}{n_s} \sum_{p=1}^{n_s} \frac{\mathscr{S}[\tilde{y}(\mathbf{x}^p) \leq 0] f_{\mathbf{X}}(x^p)}{f^*_{\mathbf{X}}(x^p)} \tag{11}$$

where, n_s is sample size of the simulation. In the above equation, $\mathscr{S}[\,.\,]$ is a discrete indicator function with binary output (i.e. either 0 or 1) based on the satisfaction of the condition stated in the third bracket. Additionally, $f_{\mathbf{X}}(x)$ is the joint probability density function (*pdf*) of the random variables and $f^*_{\mathbf{X}}(x)$ denotes a modified *pdf* applied as the weight function to balance the simulation in the vicinity of the most probable failure point. Readers may refer [20] for further details of this technique. A flowchart of the proposed sequential modelling is shown in Fig. 3 and the application of this method is discussed in the following section.

Numerical Results and Discussion

The proposed sequential SRSM discussed in the previous section is considered here for numerical analysis. Results obtained from this method is compared with other methods (e.g. FORM, SORM, HO-SRSM, SRSM, MCS) to

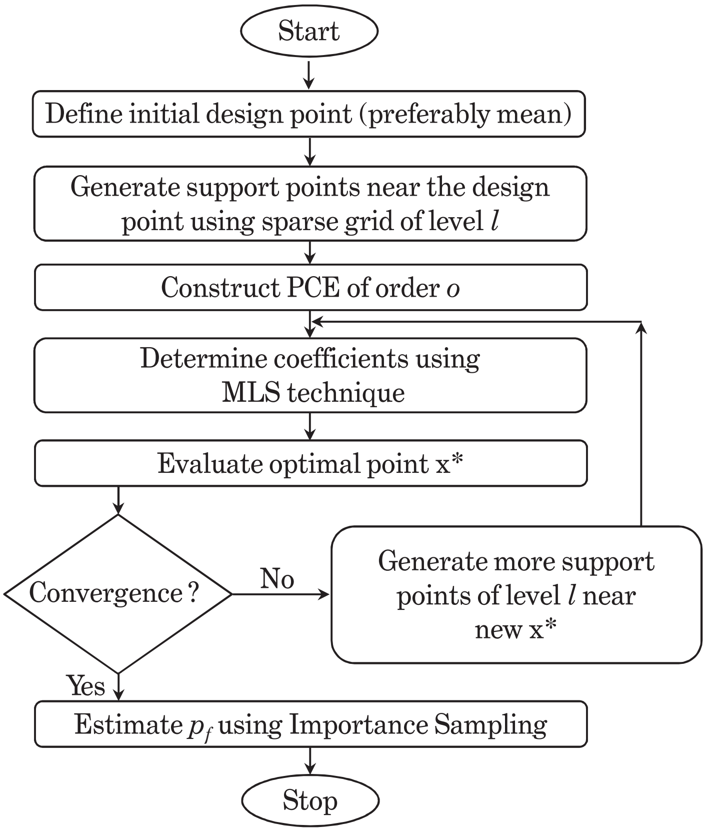

Figure 3: Flowchart of the proposed sequential SRSM

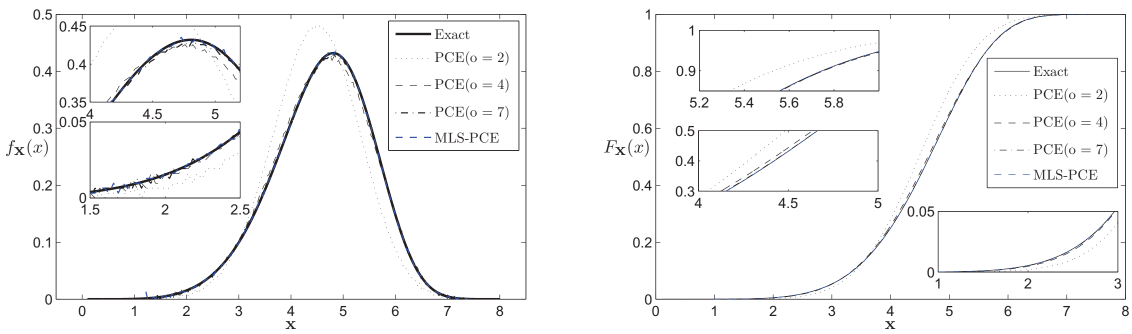

(a) **(b)**

Figure 4: Comparison of (a) *pdf* and (b) CDF of a random variable following Weibull distribution evaluated from different methods

demonstrate its efficiency and accuracy. The order of the proposed MLS based SRSM is fixed at 2 as it is sufficient to accurately capture the nature of the non-normal *pdf*. For this purpose, Weibull distribution is considered to check the adequacy of the order. The random variable is assumed to have mean and variance as 4.60 and 0.85 respectively. For MLS based PCE modelling, the effective range of [0, 8] is subdivided in 8 equidistant segments. Fig 4 shows the *pdf* and CDF of the Weibull distribution using conventional PCE of different order and propose MLS-PCE. As the order increases, conventional PCE matches with the exact value. It is noticed that an order 7 is adequate for conventional PCE to map the Weibull distribution. However, same accuracy is achieved with MLS-PCE of order 2.

With this performance of the MLS-PCE in hand, proposed sequential SRSM is tested with different benchmark problems. For this purpose, three different problems are considered from literature with different complexities. The performance of the sequential SRSM is tested vis-à-vis with other methods. Finally, a design problem involving nonlinear finite element analysis of a composite plate is presented to demonstrate the superiority of the proposed algorithm for reliability analysis.

Example 1: Franke's Test Surface

In this example, a non-algebraic bivariate performance function is considered which is given by

$$\begin{aligned} y(\mathbf{x}) \; = \; & 0.75\exp\{-0.25(9x_1-2)^2 - 0.25(9x_2-2)^2\} + 0.75\exp\left\{-\frac{(9x_1-2)^2}{49} - \frac{(9x_2-2)^2}{10}\right\} \\ & + 0.50\exp\{-0.25(9x_1-7)^2 - 0.25(9x_2-3)^2\} - 0.25\exp\{-(9x_1-4)^2 - (9x_2-7)^2\} - 0.25 \end{aligned} \tag{12}$$

where, x_1 and x_2 are independent Gaussian random variables with mean $\mu_{\mathbf{X}} = 0.40$ and standard deviation $\sigma_{\mathbf{X}} = 0.10$. The function in Eq. 12 is a modified version of the original Franke's test surface where the limit for failure is set to 0.25 [21]. It is widely considered as a benchmark exercise for testing the interpolation of scattered data. Fig. 5a shows the profile of the original surface which includes two humps (i.e. maxima) and a crater (i.e. minima).

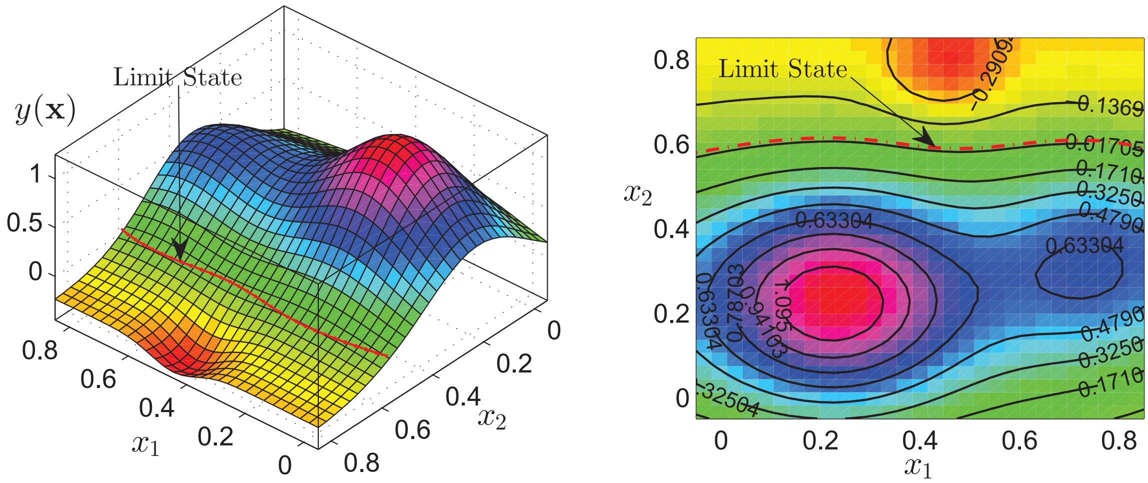

(a) **(b)**

Figure 5: (a) Surface plot and (b) contour plot of the Franke's test surface with limit state

Now, to demonstrate the sequential response surface, Franke's test surface is simplified by cutting the surface using an imaginary plane through the mean value of the random variable x_1 as shown in Fig. 6. This, in fact, reduces the test surface to a 1D function of the random variable x_2. As stated in the flowchart (Fig. 3), the process commences from the mean of the random variable (i.e. μ_{x_2}) which is assumed as the initial design point. The support points using Clenshaw-Curtis sparse grid of level l are generated around this design point. Lower and upper bounds of the support points are adopted using a prior guess which is sufficient enough to accommodate the limit state condition (i.e. $y(\mathbf{x}) = 0$). The sequential SRSM employs Hermite polynomials which are in Gaussian space. Hence, the limits for the random variable x_2 in the standard normal space is considered to be $[-5\ 5]$. Based on the sparse grid level $l = 2$, three equidistant support points are generated in the first iteration such that the points are placed on the limits and the mean as shown in Fig. 6a. In this context, it may be noted that support points for ξ_2 are generated in the standard normal space and converted into its original space defined by x_2. Using these three points, an approximated surface with PCE of order $o = 2$ is constructed using MLS technique as discussed earlier. Eq. 7 is optimized for determining the next optimal location (i.e. new design point) for generating more support points. In

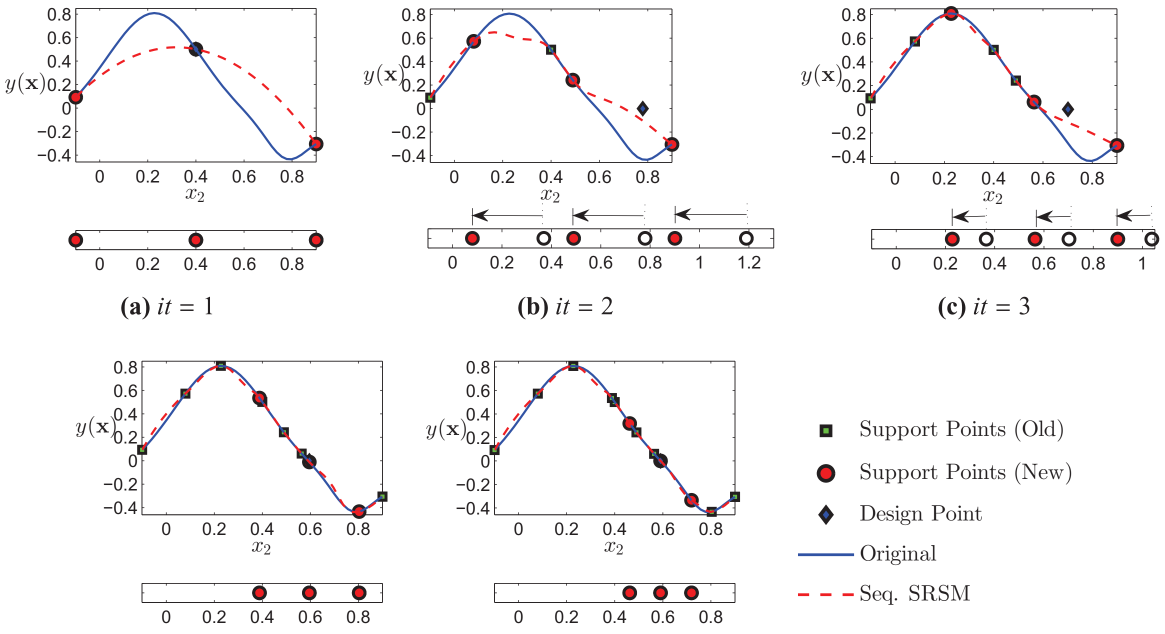

(a) *it* = 1 **(b)** *it* = 2 **(c)** *it* = 3

(d) *it* = 4 **(e)** *it* = 5

Figure 6: Sequential generation of the support points using the sparse grid scheme

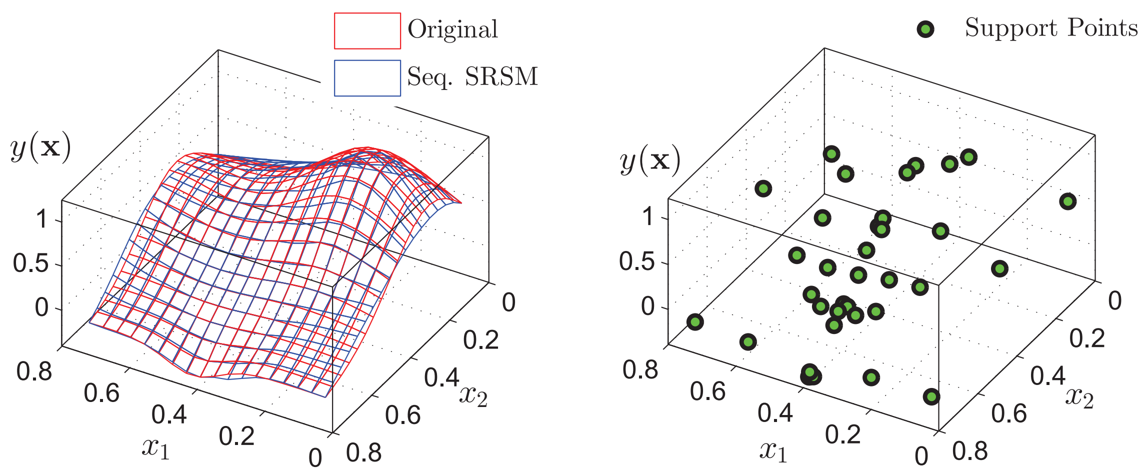

(a) **(b)**

Figure 7: Plot of the approximate surface from (a) sequential SRSM and (b) the support points generated by the sparse grid scheme

the following iteration $it = 2$, additional support points are generated around the new design point using $l = 2$. Here, the extent (i.e. difference between the bounds) of the new support points is reduced from the previous one by a factor $\lambda < 1$ so that more points are segregated near the design point. In this case, $\lambda = 0.82$ is adopted which is observed to give quick convergence. The positions of these new support points are shown in Fig. 6b. It can be observed that the position of one support point lies beyond the domain $[-5\ 5]$. Therefore, the position of all new support points are shifted uniformly to fit within the given limits. This uniform shifting of the positions is done to maintain the symmetry of the new support points. However, if the initial guess on bounds does not contain the

Table 1: Comparison of the probability of failure for the Franke's function

Method	Order	p_f	Function Calls	Error (%)	Remark
MCS	-	0.02459	10^6	-	-
FORM	-	0.02714	36	10.37	-
SORM	-	0.02386	56	2.97	-
SRSM	4	0.03489	25	41.89	-
	6	0.03142	49	27.78	-
	8	0.02968	81	20.70	-
	10	0.02812	121	14.36	-
HO-SRSM	-	0.02647	70	7.65	$o = [6, 7]$
Seq. SRSM	2	0.02446	36	0.53	$l = 2^{(for\ it=1,2)}$ and $l = 1^{(for\ it=3,4)}$

limit state [i.e. $y(\mathbf{x}) = 0$], the bounds may be suitably readjusted to incorporate the failure region. Once the position of the new support points are shifted as shown in Fig. 6b, Eq. 4 is solved to determine the unknown coefficients at these positions. The approximated surface is improved using the old as well as the new support points. Again the optimization is executed to determine the next location for $it = 3$. In every successive iteration, new support points are accommodated by further narrowing their extent by reducing the factor λ from $it = 3$ onwards. This eventually helps is concentrating the support points at the failure region for fast convergence. In this case, the convergence is achieved in 5 iterations requiring 15 function calls. However, only 13 actual function calls are executed because in $it = 2$ and 3 have two common points. Fig. 6e shows the performance function (i.e. original and proposed) after convergence.

Using this sequential development of response surface, Franke's function is modelled with two different sparse grid levels. Iteration 1 and 2 used $l = 2$ while all other it used $l = 1$ until convergence. This leads to an total of 4 iterations and 36 actual function calls. Fig. 7 shows the approximation achieved and the support points generated in the proposed sequential SRSM for the bivariate Franke's test surface. The example is also solved by different methods for reliability estimation and the results from these methods are summarized in Table 1. In this study, MCS is assumed to be most accurate estimation of probability of failure which gives $p_f = 0.02459$ with one million samples (i.e. $n_s = 10^6$). The solution using FORM and SORM converges after 36 and 56 function calls and p_f estimated from both these methods are 0.02714 and 0.02386 with 10.37% and 2.97% error, respectively. Additionally, it was observed that the initial choice of design point in FORM and SORM (e.g. [0.2 0.2]) may lead to difficulty in achieving convergence and eventually yields erroneous results. Conventional SRSM is executed with PCE of order 4, 6, 8 and 10 for both the variables. It requires 25 to 121 function calls for estimating p_f with error 14.36–41.89% as shown in the Table 1. HO-SRSM [9] solves the limit state with the order $o = 6$ and 7 for random variables x_1 and x_2, respectively which gives $p_f = 0.02647$ (i.e. 7.65% error) with 70 function calls. Almost half number of function calls are demanded to perform the proposed sequential SRSM to get $p_f = 0.02446$ which is fairly accurate as the error is 0.53%.

Example 2: Fortini's Clutch

Next example in this study is Fortini's clutch assembly which consists of a hub and four roller bearings placed in a cage as shown in Fig. 8. Its application for reliability methods is discussed by Lee and Kwak [22]. The clutch is designed for the overturning based on the contact angle θ as shown in the Fig. 8. This angle θ is formed by a vertical axis passing through center of hub and a line connecting the centers of the opposite roller bearings and the hub center. Thus, the limit state can be defined as

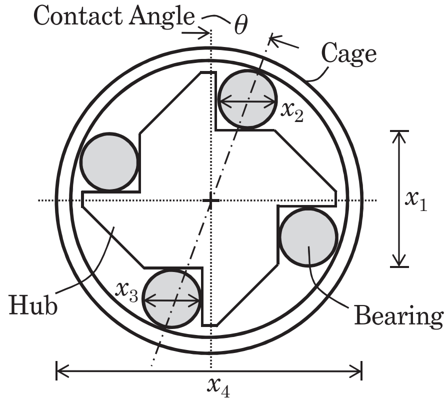

Figure 8: Fortini's clutch assembly

$$y(\mathbf{x}) = \underbrace{\arccos\left[\frac{x_1 + \frac{1}{2}(x_2 + x_3)}{x_4 - \frac{1}{2}(x_2 + x_3)}\right]}_{\theta} - 0.08726 \tag{13}$$

where, x_1, x_2, x_3 and x_4 are independent random variables with statistical properties mentioned in Table 2. In order

Table 2: Statistical properties of the variables in Fortini's clutch assembly

Random variables	Mean (μ_X)	Standard deviation (σ_X)	Distribution
x_1(mm)	55.29	7.93×10^{-2}	Beta
x_2(mm)	22.86	4.30×10^{-3}	Gaussian
x_3(mm)	22.86	4.30×10^{-3}	Gaussian
x_4(mm)	101.60	7.93×10^{-2}	Rayleigh

to avoid overturning of the clutch and operate smoothly, the contact angle θ must lie within 5° (i.e. 0.08726 radian). Table 3 summarizes the probability of failure, error and number of function calls obtained from various methods. The gradient based methods (i.e. FORM and SORM) diverge [22] and are unable to estimate the probability of failure. MCS estimates the $p_f = 0.00130$ with a sample size of 10^5. For this example, conventional SRSM computes probability of failure using orders $o = 3$, 5 and 7 for all random variables which yields 0.00116, 0.00120 and 0.00118, respectively. It suffers from inaccuracies of 7.69% to 10.77% in spite of using significant number of support points (i.e. $n_e = 256$, 1296 and 4096, respectively). The problem is further solved using HO-SRSM where the order of the polynomials in Eq. 13 are determined to be 5, 2, 2 and 5 respectively. This consumes 192 support points to give $p_f = 0.00094$ of error nearly 28%. Finally, p_f is estimated using the proposed method for different values of sparse grid level l as shown in Table 3. A mixed usage of l is demonstrated where the initial few iterations adopt higher value of l as compared to the later iterations. Four cases are shown in the Table 3, including three cases where $l = 2$ is considered for initial few iterations and then, level l is reduced to 1 until convergence is achieved. From this table, it may be noticed that the accuracy decreases with the decrease in level of sparse grid. It is obvious as there are less number of points in lower level over the effective range leading to inaccurate meta modelling. However, as the level is increased (i.e. more support points), algorithm demands more computational cost which may impose serious restrictions for large problems. Thus, there must be a tradeoff between the level and the accuracy that varies from problem to problem and demands an intermittency criteria to choose an optimal level for the specific problem. In this context, $l = 2$ in first two iterations followed by $l = 1$ in successive iterations is found to produce optimal results.

Table 3: Estimation of probability of failure p_f using MCS and the proposed sequential SRSM for different sparse grid levels l

Method	Order	p_f	Error (%)	Function Calls	Remark
MCS	-	0.00130	-	10^5	-
FORM	-	-	-	-	-
SORM	-	-	-	-	-
SRSM	3	0.00116	10.77	256	-
	5	0.00120	7.69	1296	-
	7	0.00118	9.23	4096	-
HO-SRSM	-	0.00094	27.77	192	$o = [5, 2, 2, 5]$
Seq. SRSM	2	0.00125	3.85	164	$l = 2^{(for\ it = 1,\dots,4)}$
	2	0.00130	0.00	132	$l = 2^{(for\ it = 1,2,3)}$; $l = 1^{(for\ it = 4)}$
	2	0.00124	4.62	100	$l = 2^{(for\ it = 1,2)}$; $l = 1^{(for\ it = 3,4,5)}$
	2	0.00116	10.66	77	$l = 2^{(for\ it = 1)}$; $l = 1^{(for\ it = 2,\dots,5)}$

Example 3: Non-differentiable Function

In this example, a hypothetical limit state is examined where it is expressed as [21]

$$y(\mathbf{x}) = 35 - \sum_{i=1}^{2} x_i^2 - \sum_{j=3}^{6} x_j - \frac{x_7 x_8 x_9}{\max(1, x_{10})} \tag{14}$$

In the above limit state, max(.) gives the largest value among the set in the first bracket. This leads to non-

Table 4: Random variables in the non-differentiable function example

Random variables	Mean (μ_X)	Standard deviation (σ_X)	*pdf*
x_1, x_2	-0.200	1.200	Gaussian
x_3	2.500	0.400	Gaussian
x_4, x_5, x_6	2.500	1.400	Gaussian
x_7	1.000	1.000	Gaussian
x_8	1.230	0.350	Gaussian
x_9	0.980	0.023	Gaussian
x_{10}	2.000	1.000	Gaussian

differential nature of the performance function that restricts the use of any gradient based reliability analysis (e.g. FORM, SORM) [21]. Thus, for this case, the random variable x_{10} is responsible for discontinuity in the limit state. Table 4 shows the statistical properties of the five uncorrelated random variables in this case. For checking the accuracy, results from MCS with 10^6 simulations is presented in Table 5. Conventional SRSM is performed with order o = 2 and 3 for all the random variables which demands 59046 and 1048576 support points, respectively. This makes the process very expensive as the later (i.e. SRSM with o = 3) requires more function calls than MCS. Besides constant order of PCE for all the variables as in the fist two cases, SRSM with variable orders are also tried

Table 5: Comparison of the probability of failure for the non-differentiable function example

Method	Order	p_f	Function Calls	Error (%)	Remark
MCS	-	0.000396	10^6	-	-
FORM	-	-	-	-	-
SORM	-	-	-	-	-
SRSM	2	0.000422	59046	6.57	-
	3	0.000417	1048576	5.30	-
	-	0.000400	19440	1.01	$o = [2, 2, 1, 1, 1, 1, 2, 2, 2, 4]$
HO-SRSM	-	0.000430	1804	8.59	$o = [2, \ldots, 2, 4]$
Seq. SRSM	2	0.000387	504	2.27	$l = 2^{(for\ it = 1,2)}$ and $l = 1^{(for\ it = 3,4)}$

and tabulated above. Different orders of these PCE for ten random variables are shown in the third case of SRSM. The result obtained in this case with 19440 function calls has 1.01% error. Although the result is fairly accurate, the computation cost is significantly high. HO-SRSM is further used to calculate the probability of failure which is estimated to be 0.000430 (i.e. 8.59%) with 1804 support points, consuming relatively less computation cost. This results in huge reduction in n_e and enhanced accuracy as compared to previously discussed case of $o = 2$ and 3. The observation clearly indicates that in full grid schemes, the unnecessary support points might reduce its efficiency. Application of sequential SRSM further reduces the computational effort to 504 function calls which is nearly 72% reduction from that in HO-SRSM. Additionally, the accuracy of the proposed method is also well within acceptable limits.

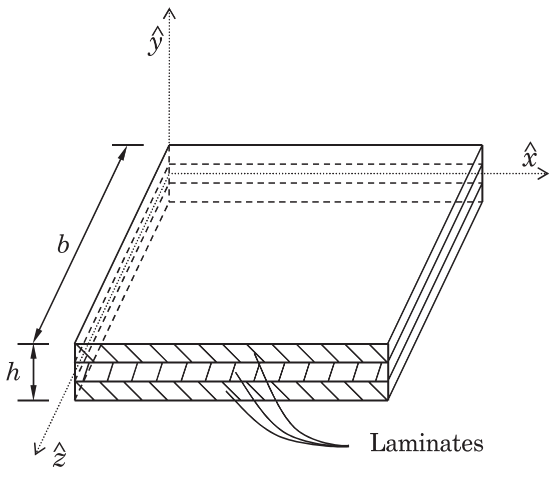

Figure 9: Composite plate

Example 4: Geometrically Nonlinear Composite Plate

Finally, the reliability based design of a carbon-epoxy composite plate is carried out to study the performance of the proposed sequential SRSM. The composite plate, as shown in Fig. 9, consists of laminates stacked in proper sequence with different orientations. In the present work, geometrically nonlinear composite plate is studied for reliability analysis where the properties of the laminates are adopted to be similar with identical thickness. The laminates in the plate are analyzed using first order shear deformation theory (FSDT) which is based on the assumption that transverse normal is allowed to rotate. This, helps to include transverse shear strains in equilibrium equation and thus, the displacement field is given as [23]

$$\left.\begin{aligned} u(\hat{x},\hat{y},\hat{z}) &= u_0(\hat{x},\hat{y}) + \hat{z}\phi_{\hat{x}}(\hat{x},\hat{y}) \\ v(\hat{x},\hat{y},\hat{z}) &= v_0(\hat{x},\hat{y}) + \hat{z}\phi_{\hat{y}}(\hat{x},\hat{y}) \\ w(\hat{x},\hat{y},\hat{z}) &= w_0(\hat{x},\hat{y}) \end{aligned}\right\}. \tag{15}$$

In the above equation, mid-plane displacements u_0, v_0 and w_0 are associated to $\hat{x}$, $\hat{y}$ and $\hat{z}$ directions, respectively. The rotation with respect to transverse normal denoted by $\phi_{\hat{x}}$ is about $\hat{y}$ and similarly, $\phi_{\hat{y}}$ is about $\hat{x}$. Using thin plate condition where rotations are determined by slopes of the transverse deflection and applying the von-Karman assumptions in Eq. 15, yields [23]

$$\begin{bmatrix} \varepsilon_{\hat{x}\hat{x}} \\ \varepsilon_{\hat{y}\hat{y}} \\ \gamma_{\hat{x}\hat{y}} \end{bmatrix} = \begin{bmatrix} \varepsilon^m_{\hat{x}\hat{x}} \\ \varepsilon^m_{\hat{y}\hat{y}} \\ \gamma^m_{\hat{x}\hat{y}} \end{bmatrix} + \hat{z} \begin{bmatrix} \varepsilon^f_{\hat{x}\hat{x}} \\ \varepsilon^f_{\hat{y}\hat{y}} \\ \gamma^f_{\hat{x}\hat{y}} \end{bmatrix} \tag{16}$$

$$\gamma = \begin{bmatrix} \gamma_{\hat{x}\hat{z}} \\ \gamma_{\hat{y}\hat{z}} \end{bmatrix} \tag{17}$$

where, $\gamma_{\hat{x}\hat{z}}$ and $\gamma_{\hat{y}\hat{z}}$ represents shear strains. In Eq. 16, the superscripts m and f denotes membrane and flexural components, respectively. Geometric nonlinearity caused by large deformations gives rise to additional higher order terms in the strain field. This modifies the membrane strain to [23]

$$\left.\begin{aligned} \varepsilon^m_{\hat{x}\hat{x}} &= u_{0,\hat{x}} + \tfrac{1}{2}(w_{0,\hat{x}})^2 \\ \varepsilon^m_{\hat{y}\hat{y}} &= v_{0,\hat{y}} + \tfrac{1}{2}(w_{0,\hat{y}})^2 \\ \varepsilon^m_{\hat{x}\hat{y}} &= u_{0,\hat{y}} + v_{0,\hat{x}} + w_{0,\hat{x}}\, w_{0,\hat{y}} \end{aligned}\right\}. \tag{18}$$

Thus, the constitutive equation for a laminate is expressed as [23]

$$\begin{Bmatrix} \sigma_1 \\ \sigma_2 \\ \tau_{12} \\ \tau_{23} \\ \tau_{13} \end{Bmatrix} = \begin{bmatrix} Q_{11} & Q_{12} & 0 & 0 & 0 \\ Q_{21} & Q_{22} & 0 & 0 & 0 \\ 0 & 0 & Q_{66} & 0 & 0 \\ 0 & 0 & 0 & Q_{44} & 0 \\ 0 & 0 & 0 & 0 & Q_{55} \end{bmatrix} \begin{Bmatrix} \varepsilon_1 \\ \varepsilon_2 \\ \gamma_{12} \\ \gamma_{23} \\ \gamma_{13} \end{Bmatrix} \tag{19}$$

where, Q_{ij} represents the plane stress reduced stiffness coefficients. In Eq. 19, these coefficients are defined in the material axes of the laminate which can be transformed into the global axes by

$$\breve{Q} = [T][Q][T]' \tag{20}$$

where, $[T]$ is the transformation matrix. The orthotropic laminate, after this transformation, acts as anisotropic which also include coupling terms. Thus, the constitutive equation for a composite plate by adding the laminates to get a equivalent single layer is given as

$$\begin{bmatrix} [N] \\ [M] \end{bmatrix} = \begin{bmatrix} [A] & [B] \\ [B] & [D] \end{bmatrix} \begin{bmatrix} \varepsilon^m \\ \varepsilon^f \end{bmatrix} \tag{21}$$

where, $[N]$ and $[M]$ are the force and moment resultants, respectively. Also, $[A]$ is the extensional stiffness matrix, $[B]$ represents the bending-extension coupling stiffness matrix and $[D]$ denotes the bending stiffness matrix.

Here, total Lagrangian incremental formulation is adopted for developing the geometric nonlinear equilibrium equation [23]. Hence, the virtual work equation of undeformed plate with volume V and area a is given as

$$\int_V (d\varepsilon^T \sigma\, dV) = \int_V (\rho\, du^T g\, dV) + \int_A (du^T p\, da) \tag{22}$$

where, $d\varepsilon$ is the virtual Green strain vector, du gives the virtual displacement, σ represents Piola-Kirchoff stress vector, ρ is the mass density of the material, g is the body force per unit mass and p denotes the pressure applied on the plate. The displacement field can be discretized using finite elements which is given by

$$\bar{u} = \sum_{i=1}^{n_n} [\Omega_i I] q_i \tag{23}$$

where, I is the identity matrix, Ω_i denotes the shape function for any arbitrary node i, $q_i = [u_i\ v_i\ w_i\ \phi_{xi}\ \phi_{yi}]^T$ gives the nodal displacements. Extending the above equation for the complete thickness yields the elemental nonlinear equilibrium equation as

$$\psi(q) = \sum_{i=1}^{n_e} \left[\int_a ([\check{B}]'\, \bar{\sigma}\, da) - \{\bar{P}\}_e \right] = 0 \tag{24}$$

where, $\check{B}$ denotes the strain-displacement matrix with nonlinear terms, $\psi(q)$ represents the summation of external and internal forces, $\bar{\sigma}$ gives the force and moment resultant and $\{\bar{P}\}_e$ is the total external force at the element level. The nonlinear equilibrium equation can be evaluated by solving Eq. 24 with respect to the displacement vector q. This yields the expression in the terms of displacement, force and stiffness. In the present study, Newton-Raphson iterative technique [23] is used for solving this nonlinear equilibrium equation.

Using this finite element model of a geometrically nonlinear plate, fragility analysis is carried out for the reliability based design. Table 6 shows the statistical properties of the random variables used in this example. In this study, modified Tsai-Hill failure [24] criterion is adopted to define the limit state. This criterion is an extension of the von-Mises distortion energy theory [25]. The limit state based on the modified Tsai-Hill failure index $\mathscr{F}$ is expressed as

$$y(\mathbf{x}) = 1 - \underbrace{\left\{ \left(\frac{\sigma_{11}}{X}\right)^2 + \left(\frac{\sigma_{22}}{Y}\right)^2 - \left(\frac{\sigma_{11}\sigma_{22}}{X^2}\right) + \left(\frac{\sigma_{12}}{T_{12}}\right)^2 \right\}}_{\mathscr{F}} \tag{25}$$

where, σ_{11}, σ_{22} and T_{12} are the laminate stresses along the respective material coordinates whereas X and Y are the tensile and compressive strengths. As shown in the Eq. 25, the limit state reflects the condition when the failure index $\mathscr{F}$ of any laminate exceeds unity [24].

Table 6: Statistical parameters and distribution of the random variables in the composite plate

Random Variables	Units	Mean	cov (%)	*pdf*	Parameters	
$\nu_{12} \rightarrow x_1$	-	0.281	7.5	Lognormal	-	-
$G_{12} \rightarrow x_2$	GPa	4.5	8.8	Lognormal	-	-
$X_t \rightarrow x_3$	GPa	2.409	6.7	Lognormal	-	-
$X_c \rightarrow x_4$	GPa	1.148	18.1	Lognormal	-	-
$T_{12} \rightarrow x_5$	GPa	0.083	5	Lognormal	-	-
$E_1 \rightarrow x_6$	GPa	154.9	5.9	Weibull	158.820	21.6
$E_2 \rightarrow x_7$	GPa	8.7	9.5	Weibull	9.055	12.9
$Y_t \rightarrow x_8$	GPa	0.046	20	Weibull	0.050	5.7
$Y_c \rightarrow x_9$	GPa	0.196	15.3	Weibull	0.209	7.7

A square carbon-epoxy composite plate is considered of dimension 1×1 m and thickness 0.010 m. The plate is simply supported in all four sides with uniformly distributed load (UDL = 0.090 MPa) acting downwards. The laminates are placed with orientation [0°/90°/0°]. To perform the finite element analysis, quadrilateral nine noded element with a mesh size 8×8 is used. The random variables in this study are elastic modulus E_1 and E_2, shear modulus G_{12}, Poisson's ratio ν_{12} and strength parameters X_t, X_c, Y_t, Y_c and T_{12}. Their statistical parameters and *pdf* types are adopted from Sasikumar *et al.* [24] and mentioned in Table 6. Using these parameters, the reliability of the plate against modified Tsai-Hill failure criterion is evaluated by all the methods described in previous examples and the results are tabulated in Table 7. As usual, the MCS is conducted with 10^4 samples and is considered as the benchmark for further analysis. Gradient based methods (i.e. FORM and SORM) gives satisfactory results with 220 and 751 function calls respectively. The probability of failure estimated for these two cases have error around 3.1% and 2.99%. A marginal improvement in second order method is noticed. However, the quality of the results largely depends on the initial guess which is known drawback of the gradient based techniques. With these results

Table 7: Comparison of the probability of failure for the nonlinear composite plate

Method	Order	p_f	Function Calls	Error (%)	Remark
MCS	-	0.1906	10^4	-	-
FORM	-	0.1965	220	3.10	-
SORM	-	0.1963	751	2.99	-
SRSM	-	0.2187	1280	14.74	$o = [1, 1, 1, 1$ $1, 1, 1, 4, 1]$
	-	0.2632	1536	38.09	$o = [1, 1, 1, 1$ $1, 1, 1, 5, 1]$
HO-SRSM	-	0.1900	3324	0.31	$o = [2, 2, 2, 2$ $2, 5, 3, 5, 2]$
Seq. SRSM	2	0.1975	456	3.64	$l = 2^{(for\ it = 1,2)}$ and $l = 1^{(for\ it = 3,4,5)}$

in hand, SRSM and its modified versions are tried. First, the conventional SRSM is tried with order 2 and 3 that need 19683 and 262144 function calls. These are well above the function calls required for MCS. As each function call needs to solve nonlinear finite element code to check the failure criterion involving significant computation time, this method for reliability estimation of the nonlinear composite plate is not feasible. Moreover, the results from the SRSM have 14.74% and 38.09% error for two different combination of orders of random variables which are not satisfactory at all. Once the performance of conventional SRSM is studied, HO-SRSM is tried with different order. It is found that it converged with $p_f = 0.19$ that has 0.31% error with 3324 function calls. Finally, proposed sequential SRSM is used to study the failure. It is noticed that the proposed method with $l = 2$ in first two iterations followed by $l = 1$ converges after 5 iterations with error less than 3.84%. It requires 456 function calls which is more than FORM but well below that required for SORM and HO-SRSM. This clearly justifies the superiority of the proposed method for actual design problems involving large finite element models.

Summary

An efficient reliability analysis using sequential development of SRSM is demonstrated here. In this process, the proposed MLS based SRSM is formed with Clenshaw-Curtis sparse grid scheme with equidistant support points in each successive iterations. The order of the polynomials and the level of the sparse grid are adjusted in every iteration that offers significant flexibility to optimize computational cost while compromising with the accuracy of the end result. In this context, different optimization tool may be adopted as the proposed imposes no restriction. Using this sequential SRSM, different benchmark problems are solved to demonstrate its performance. The numerical study presented in this paper clearly demonstrates that level of accuracy and computation cost involved in the proposed method. It may be concluded that the proposed sequential SRSM offers appreciable accuracy at an optimal computational cost. Overall, it proves to be an effective tool for reliability analysis for problems with large dimension and other complexities.

With simple modifications, the proposed method can be adopted for problems with multiple performance function and/or multiple failure points and uncertainty quantification. Authors wish to address these issues in their future work.

References

[1] Myers, R. H., Montgomery, D. C. and Anderson-Cook, C. M. (2009) *Response Surface Methodology: Process and Product Optimization Using Designed Experiments*, 3rd edn. John Wiley & Sons, Hoboken, New Jersey, USA.

[2] Ghanem, R. G. and Spanos, P. D. (1991) *Stochastic Finite Elements: A Spectral Approach*, Springer-Verlag New York, USA.

[3] Haldar, A. and Mahadevan, S. (2000) *Reliability Assessment using Stochastic Finite Element Analysis*, John Wiley & Sons, Inc., New York, USA.

[4] Xiu, D. and Karniadakis, G. E. (2003) Modeling uncertainty in flow simulations via generalized polynomial chaos, *Journal of Computational Physics* **187** (1), 137 – 167.

[5] Kameshwar, S., Rathi, A. K. and Chakraborty, A. (2012) A Modified Gradient Based Reliability Analysis for Nonlinear Nonalgebraic Limit States Using Polynomial Chaos Expansion, *Proceedings of* 4^{th} *International Congress on Computational Mechanics and Simulation*, Hyderabad, India, December 10–12.

[6] Isukapalli, S. S. (1999) *Uncertainty Analysis of Transport-Transformation Models*, Ph.D. dissertation. Rutgers, The State University of New Jersey.

[7] Sudret, B. and Der Kiureghian, A. (2002) Comparison of Finite Element Reliability Methods, *Probabilistic Engineering Mechanics* **17** (4), 337 – 348.

[8] Choi, S.-K., Grandhi, R. V. and Canfield, R. A. (2004) Structural Reliability under Non-Gaussian Stochastic Behavior, *Computers & Structures* **82** (13–14), 1113 – 1121.

[9] Gavin, H. P. and Yau, S. C. (2008) High-Order Limit State Functions in the Response Surface Method for Structural Reliability Analysis, *Structural Safety*, **30** (2), 162 – 179.

[10] Blatman, G. and Sudret, B. (2010) Reliability Analysis of a Pressurized Water Reactor Vessel using Sparse Polynomial Chaos Expansions, *Reliability and Optimization of Structural Systems*, 9 – 16, CRC Press.

[11] Xiong, F., Chen, W., Xiong, Y. and Yang, S. (2011) Weighted Stochastic Response Surface Method Considering Sample Weights, *Structural and Multidisciplinary Optimization*, **43** (6), 837 – 849.

[12] Xiong, F., Liu, Y., Xiong, Y. and Yang, S. (2012) A Double Weighted Stochastic Response Surface Method for Reliability Analysis, *Journal of Mechanical Science and Technology*, **26** (8), 2573–2580.

[13] Hu, C. and Youn, B. D. (2011) Adaptive-Sparse Polynomial Chaos Expansion for Reliability Analysis and Design of Complex Engineering Systems, *Structural and Multidisciplinary Optimization*, **43** (3), 419–442.

[14] Rathi, A. K. and Chakraborty, A. (2016) Reliability-Based Performance Optimization of TMD for Vibration Control of Structures with Uncertainty in Parameters and Excitation, *Structural Control and Health Monitoring*.

[15] Most, T. and Bucher, C. (2005) A Moving Least Squares weighting function for the Element-free Galerkin Method which almost fulfills essential boundary conditions, *Structural Engineering and Mechanics* **21** (3), 315 – 332.

[16] MATLAB® version 7.13.0.564 (R2011b), The MathWorks Inc., Natick, Massachusetts, USA.

[17] Holtz, M. (2011) Sparse Grid Quadrature, In *Sparse Grid Quadrature in High Dimensions with Applications in Finance and Insurance* (51–76). Springer Berlin Heidelberg, Berlin, Heidelberg.

[18] Clenshaw, C. W. and Curtis, A. R. (1960) A Method for Numerical Integration on an Automatic Computer, *Numerische Mathematik*, **2** (1), 197 – 205.

[19] Klimke, A. and Wohlmuth, B. (2005) Computing Expensive Multivariate Functions of Fuzzy Numbers using Sparse Grids, *Fuzzy Sets and Systems*, **154** (3), 432 – 453.

[20] Melchers, R. E. (1989) Importance Sampling in Structural Systems, *Structural Safety*, **6** (1), 3 – 10.

[21] Chowdhury, R., Rao, B. N. and Prasad, A. M. (2009) High-Dimensional Model Representation for Structural Reliability Analysis, *Communications in Numerical Methods in Engineering*, **25** (4), 301 – 337.

[22] Lee, S. H. and Kwak, B. M. (2006) Response Surface Augmented Moment Method for Efficient Reliability Analysis, *Structural Safety* **28**, 261 – 272.

[23] Reddy, J. N. (2004) *Mechanics of Laminated Composite Plates and Shells: Theory and Analysis*, CRC Press.

[24] Sasikumar, P., Suresh, R. and Gupta, S. (2014) Analysis of CFRP Laminated Plates with Spatially Varying Non-Gaussian Inhomogeneities using SFEM, *Composite Structures* **112**, 308 – 326.

[25] Mohite, P. M. *Composite Materials and Structures*, National Programme on Technology Enhanced Learning (NPTEL), Accessed on: 16 May 2016. `http://www.nptel.ac.in/courses/101104010/`